

Vibration control of offshore wind turbine using RSM and PSO-optimized Stockbridge damper under the earthquakes

Mohammad S. Islam^{1a}, Jeongyun Do^{*2} and Dookie Kim^{1b}

¹Civil and Environmental Engineering, Kunsan National University, 558 Daehak-ro, Gunsan-si 54150, Republic of Korea

²Industry-University Cooperation Foundation, Kunsan National University, 558 Daehak-ro, Gunsan-si 54150, Republic of Korea

(Received June 5, 2017, Revised January 16, 2018, Accepted January 19, 2018)

Abstract. In this inquisition, a passive damper namely Stockbridge Damper (SBD) has been introduced to the field of vibration control of Offshore Wind Turbine (OWT) to reduce the earthquake excitations. The dynamic responses of the structure have been analyzed for three recorded earthquakes and the responses have been assessed. To find an optimum SBD, the parameters of damper have been optimized using Response Surface Methodology (RSM) based on Box-Behnken Design (BBD) and Particle Swarm Optimization (PSO). The influence of the design variables of SBD such as the diameter of messenger cable, the length of messenger cable and logarithmic decrement of the damping has been investigated through response variables such as maximum displacement, RMS displacement and frequency amplitude of structure under an artificially generated white noise. After that, the structure with optimized and non-optimized damper has been analyzed with under the same earthquakes. Moreover, the comparative results show that the structure with optimized damper is 11.78%, 18.71%, 11.6% and 7.77%, 7.01%, 10.23% more effective than the structure with non-optimized damper with respect to the displacement and frequency response under the earthquakes. The results show that the SBD can obviously affect the characteristics of the vibration of the OWT and RSM based on BBD and PSO approach can provide an optimum damper.

Keywords: Stockbridge damper; vibration control; offshore wind turbine; response surface methodology; Box-Behnken design; particle swarm optimization; multiobjective optimization

1. Introduction

1.1 Background and purpose

Among many of renewable energy sources, the offshore wind turbine (OWT) is a potential one. Currently, it has received more investment for its' eco-friendly and low-cost energy production feature. Moreover, with the development of OWTs, these structures are becoming higher, slender and also becoming more susceptible to the vibrations. The vibrations in the OWT usually come from wave, wind, ice, earthquake, and so on. Among these, earthquake loads are more dynamic in nature and can cause of structural failure as well as lose of properties (Wang and Li 2013). The consideration of earthquake loads for offshore structures, which is installed in the seismic prone area has greater importance than the other external loads (Lee *et al.* 2015).

Passive vibration control system is one of the famous systems for its economic feature and robust activity. Mousavi *et al.* (2012) has proposed a tuned liquid column gas damper (TLCGD) to reduce the seismic induced vibrations of steel jacket platforms. To increase damping in an OWT, a toggle brace system has proposed by Brodersen

and Hogsberg (2014). Jeon *et al.* 2013, Jaksic *et al.* 2015, Roderick 2012 have applied the tuned liquid damper (TLD) and tuned liquid column damper (TLCD) to minimize the wave induced vibrations of floating wind turbines respectively. Alkimm *et al.* (2016) has studied on the reduction of vibrations of wind turbines using TLCD by the stochastic analysis under generated random excitations. Rahman *et al.* (2017) has studied on the vibration reduction of the offshore wind turbine by the optimized TMD under earthquake loads.

In spite of bulk of literature on vibration reduction of offshore structure, till date, it's very challenging to the researchers and engineers. In this research, a Stockbridge Damper (SBD) is suggested to suppress the vibration of the OWT system under earthquakes.

The concept of SBD has been developed by Stockbridge (1925) and it is another formation of tuned mass damper. Apparently, SBD device has been applied to control the wind-induced vibration control of transmission line (Kasap 2012, Barry 2014 and Dos Santos 2015) and pedestrian bridge (Urushadze *et al.* 2012). Navarro *et al.* (2008) have presented a general optimization design method for finding an optimum Stockbridge damper. To reduce the earthquake vibration of small structure like nuclear power plant piping system, building structure, SBD has applied successfully by Chang *et al.* (2016).

The response surface methodology (RSM) is one of the most widely-used statistical approach that is useful for analyzing the data and optimizing the processes. The RSM as a tool for optimization has used in many field such as

*Corresponding author, Ph.D. Research Professor
E-mail: arkido@gmail.com

^a Graduate Student

^b Professor

analytical chemistry (Bezerra *et al.* 2008), cement paste mix design (Soto-Pérez *et al.* 2015), cost effective mix proportioning of high strength self-compacting concrete (Khan *et al.* 2016). On the other hand, the Box-Behnken designs are experimental designs for RSM, devised by Box and Behnken (1960). It is a special 3-level design because it does not contain any points at the vertices of the experiment region. This could be advantageous when the points on the corners of the cube represent level combinations that are prohibitively expensive or impossible to test because of physical process constraints. The BBD is an alternative for the optimization of analytical methods (Ferreira *et al.* 2007). Moreover, the Particle Swarm Optimization (PSO) is a meta-heuristic optimization technique for finding an optimum damper. Sepehri *et al.* (2012) have suggested a modified particle swarm approach to solving the multi-objective optimization problem of laminated composite structures by presenting a new variation scheme for acceleration parameters and inertial weight factors of PSO. Shariatmadar and Razavi (2014) have applied the PSO to optimize fuzzy logic controller parameters.

However, to the authors' knowledge, no studies are reported to concern this issue (vibration control using SBD and SBD optimization using RSM and PSO) of the 5MW OC4 jacket supported OWT. Nevertheless, currently, this model occupies the largest number of the few installed full-scale OWT prototypes for its conspicuous capability in supporting the operational conditions of OWT.

This study aims to introduce the Stockbridge damper to the field of vibration control of Offshore Wind Turbine (OWT) to reduce the earthquake excitations. Moreover, to investigate the way of finding an optimum SBD in view of multi-objective optimization and its potential application to the vibration reduction and mitigation measure of the dynamic response of OWT subjected to earthquakes. According to its particular characteristics, an SBD model was modeled based on the Stockbridge (1925) design and theory. To find an optimum SBD, the Response Surface Methodology (RSM) based Box-Behnken Design (BBD) and Particle Swarm Optimization were employed to avoid local minimum. In the multiple optimizations, the properties of damper are considered as design variables whereas the multiple responses of the structure are considered as response variables. FEM analysis of jacket supported OWT with and without SBD is performed using OpenSees. With the aim to confirming the controlling effects of the SBD under random earthquake vibration, the three selected (El Centro, Northridge, and Tabas) earthquakes are used in this investigation before and after optimization. The performances of optimized SBD device were evaluated via the fully coupled FEM dynamic model and, the result showed the efficiency of the SBD system with respect the vibration control of OWT under the earthquake loads.

1.2 Study procedure and structure

To catch up this work easily, a flow chart on methodology has been described in Fig. 1:

Initially, model of OWT is generated considering its

properties and analyzed under the selected ground motions.

The responses of OWT like top displacement, frequency response, standard deviation of displacement, shear force, and flexural response of tower are checked. Then, a passive damper likely SBD is designed considering the design points and re-analyzed the structure with damper, and re-checked the responses. This phase name is approximation of modelling. After that, considering the design points, an optimum SBD is found based on a multi-objective optimization which is based on desirability index and PSO, respectively. This is the multi-objective optimization phase. In the final means validation phase, the responses of OWT is verified by dynamic analysis.

2. Simulated numerical model of offshore wind turbine

2.1 Equation of motion of structure with the SBD

The Offshore Wind Turbine (OWT) is multi-degree of a complicated system that consists of more degrees of flexibility with interacting devices. The studied OWT structure is shown in Fig. 2, which is assumed as a lumped mass system at each degree of freedom.

The governed equation of motion for the jacket supported OWT with the SBD is shown in Eq. (1), where the forces are considered at equilibrium state of condition for each degree of freedom.

$$[M]\{\ddot{\mathbf{u}}\} + [C]\{\dot{\mathbf{u}}\} + [K]\{\mathbf{u}\} = -[M]\{\mathbf{1}\}\ddot{u}_g \quad (1)$$

where M , C , and K are the mass, damping, and stiffness matrix of structure with $(N + 1) \times (N + 1)$ dimensions. Here, N =degrees of freedom (DOF) for the jacket support structure and 1 =DOF for the damper. The generalized coordinates of the total system are considered as

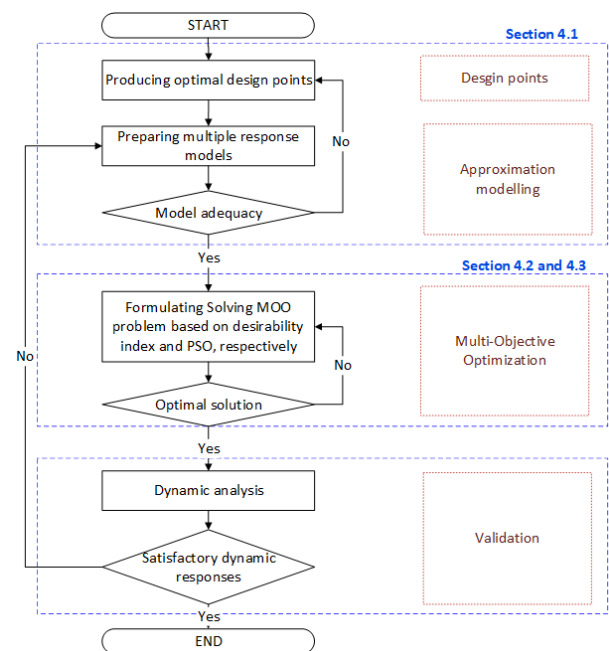


Fig. 1 Study procedure and structure

$$\{\mathbf{u}\} = [\mathbf{u}_s, \mathbf{u}_d]^T \quad (2)$$

where u_s and u_d are the displacement of i -th node of OWT and damper; $\{\mathbf{u}\}$, $\{\dot{\mathbf{u}}\}$, and $\{\ddot{\mathbf{u}}\}$ are the displacement, velocity, and acceleration vectors respectively, relative to the ground. The excitations of dynamic signal are denoted by $\{\ddot{\mathbf{u}}_g\}$. $\{\mathbf{1}\}$ is the location vector of SBD. The matrices of the mass, damping, and stiffness are as follows

$$[\mathbf{M}] = \begin{bmatrix} \mathbf{M}_{sN \times N} & \mathbf{O}_{N \times 1} \\ \mathbf{O}_{1 \times N} & \mathbf{M}_{d1 \times 1} \end{bmatrix}_{(N+1) \times (N+1)} \quad (3)$$

$$[\mathbf{C}] = \begin{bmatrix} \mathbf{C}_{sN \times N} & \mathbf{O}_{N \times 1} \\ \mathbf{O}_{1 \times N} & \mathbf{C}_{d1 \times 1} \end{bmatrix}_{(N+1) \times (N+1)} \quad (4)$$

$$[\mathbf{K}] = \begin{bmatrix} \mathbf{K}_{sN \times N} & \mathbf{O}_{N \times 1} \\ \mathbf{O}_{1 \times N} & \mathbf{K}_{d1 \times 1} \end{bmatrix}_{(N+1) \times (N+1)} \quad (5)$$

Table 1 Natural Frequency of FEM of jacket supported of offshore wind turbine

Mode	FAST (Hz)	OpenSees (Hz)
1st fore-aft mode	0.3190	0.32734
1ST Side-Side mode	0.3190	0.32734
2nd fore-aft mode	1.1944	1.1743
2nd Side-side mode	1.1944	1.1743

Table 2 Properties of the jacket supported OWT

Properties	Value/Others
Tower condition	Shutdown
Nacelle dimension	18 m × 6 m × 6 m
Total RNA mass	350000 kg
Hub height	90 m
Hub mass	56780 kg
Tower Length	68 m
Tower mass	230000 kg
Tower top and base outer diameter and thickness	4 m and 0.03 m; 5.6 m and 0.032 m
TP Dimension	68 m
Mass density of TP	1807 kg/m ³
Mass of TP	666130 kg
Braces (Jacket and Mud) outer diameter and thickness	0.8 m and 0.02 m
Jacket Mass	655700 kg
Mass density	7850 kg/m ³
Total structural mass	1901830 kg
Poisson's ratio	0.3
Platform type	Fixed platform
Constraint	Fixed
Location of damper	Top of the tower

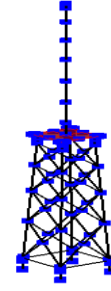
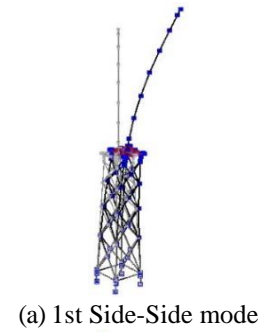


Fig. 2 Structural Model of Jacket supported offshore wind turbine



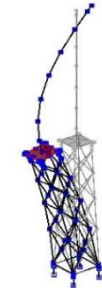
(a) 1st Side-Side mode



(b) 1st fore-aft mode



(c) 2nd Side-side mode



(d) 2nd fore-aft mode

Fig. 3 Mode shape of uncontrolled jacket supported an offshore wind turbine

2.2 Eigenvalue analysis and model validation

The eigenvalue analysis is carried out to get the natural frequencies, mode shapes, and effective modal masses of the uncontrolled structure. To check the accuracy of OWT model, the modal properties especially the natural frequency of OpenSees model are checked with the model frequencies of the FAST model. However, the corresponding modal frequencies of the structure are given in Fig. 3 and Table 1. The Table 1 illustrates that the frequencies of OpenSees finite element model seem close to the given model. In that case, our model is validated and quite perfect for further analysis.

The gravitational force is also checked for verification of model. It is found that all the reaction forces of the jacket support structure are 18.657 MN force at fixed supports without giving any other loads which are matched with the FAST model.

2.3 Structural model property

In this study, an OWT model is considered to study and the Finite Element Model (FEM) is developed following by a benchmark NREL 5 MW-OC4 jacket supported offshore wind turbine using OpenSees, and which is shown in Fig. 2.

The whole structure consists of three part such as a tower, transition piece, and jacket structure. The total height of the structure is 138 m, where the tower is 68 m and jacket is 70 m. The tower is composed of 9 elements and the element is considered as force beam-column member.

The jacket portion consists of 4 central piles, 4 levels of X-braces, mud braces, 4 legs and a transition piece (TP), respectively. Overall, the total jacket structure is modeled into 64 nodes and 112 elements through force beam-column element at OpenSees finite element software. The rotor nacelle assembly (RNA) along the hub is considered as lump mass at the top of the tower following by the NREL 5MW baseline turbine.

In this model, mesh loading is not considered because while the structure will sustain during earthquakes, that refers the structure will be sustainable for mesh loading as well as for the other environmental load. The constraint is considered as fixed to eliminate the influence of the foundation. The others geometric properties of the considered structure (Vorpahl *et al.* 2011, Song *et al.* 2013) are listed in Table 2. Here, the tower top has been chosen as the location of damper. Because the 1st mode of OWT has been governed maximum displacement and maximum modal mass of OWT.

3. Design of Stockbridge damper

3.1 Calculation of mass ratio of damper

Mass ratio is an important parameter of SBD. Inner to find a damper, it is designed based on the modal parameters of OWT. The first modal mass of OWT is considered to find the mass of the SBD. To calculate the mass ratio and optimum frequency ratio of damper, Den Hartog's (1947)

equations for tuned mass damper are utilized. Based upon the consideration of 5% structural damping ratio for all modes of uncontrolled structure, the mass ratio of damper and optimum frequency ratio is calculated by using Eqs. (6) and (7).

$$\text{Mass ratio, } \mu = \frac{8\xi_{eff}^2}{1-4\xi_{eff}^2} \quad (6)$$

$$\text{Optimum frequency ratio, } \gamma_{opt} = \frac{1}{1+\mu} \quad (7)$$

where, ξ_{eff} = Effective damping ratio of the structure for all the modes of structure.

3.2 Equation of motion of Stockbridge damper

The SBD is a combined system of tip masses and a linear spring (messenger cable) system which follows the D' Alembert's principles for its translational and rotational damping capacity. Thus SBD has two kinds of damping system such as translational and rotational. Fig. 4 shows the location, plan, and elevation of the damper. To understand easily, the plan and elevation of SBD has been separately. In elevation, damper location has been shown. The SBD has been installed at top of the tower of OWT.

The SBD, itself is a two-degree-of-freedom system. The governing equation of motion for SBD system is given in Eq. (8) at below

$$[M_d]\{\ddot{\mathbf{x}}\} + [K_d]\{\dot{\mathbf{x}}\} + [C_d]\{\mathbf{x}\} = C_d\dot{\mathbf{y}} + K_d\mathbf{y} \quad (8)$$

Eq. (8) respectively expresses the quasi-static equilibrium of the tip mass (D' Alembert's Principle) with respect to forces and moments.

The damping in SBD has been described as predominantly hysteretic (internal damping) by the Wagner *et al.* (1973).

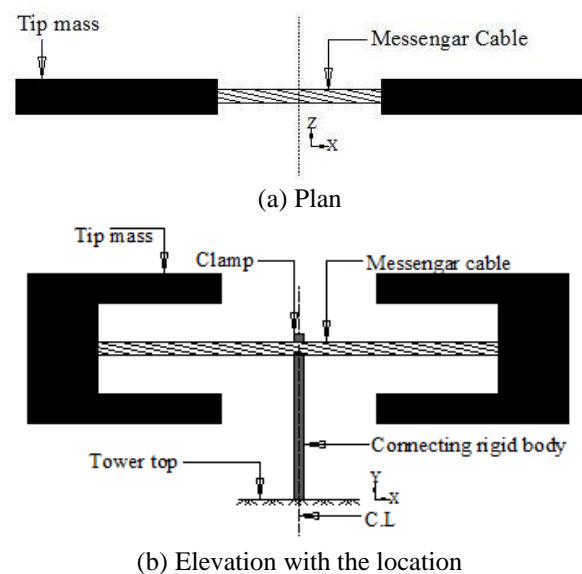


Fig. 4 Components and structure of the Stockbridge damper

Moreover, the damping in the SBD is statically hysteresis which is resulting from Coulomb (dry) friction between the individual wires of the messenger cable undergoing bending deformation (Barbieri and Barbieri 2012). Systems with statically hysteresis can be modeled by means of Jenkin elements arranged in parallel, consisting of linear springs and Coulomb friction elements. The messenger cable is a continuous system and damping takes place throughout the whole length of the cable. Under this damping system, the motion can be nearly considered as harmonic motion. From the free vibration oscillation of SBD system, Eq. (9) has been written as follows

$$[M_d]\{\ddot{x}\} + [K_d]\{\dot{x}\} + [C_d]\{x\} = 0 \quad (9)$$

where M_d , K_d , and C_d are the mass, damping and stiffness of the SBD; \ddot{x} , \dot{x} , x are acceleration, velocity and displacement of the damper.

The undamped natural frequencies of the damper system have been obtained from the following equations (Wagner *et al.* 1973)

$$\omega_1 = \left(\frac{h-a}{2m\rho} \right)^{1/2} \quad (10)$$

$$\omega_2 = \left(\frac{h+a}{2m\rho} \right)^{1/2} \quad (11)$$

$$\rho = (r/l)^2 \quad (12)$$

$$h = (1 + \rho)k_{11} + \frac{k_{22}}{l^2} - 2 \frac{k_{12}}{l} \quad (13)$$

$$a = \sqrt{h^2 - \frac{4\rho}{l^2} (k_{11}k_{22} - k_{12}^2)} \quad (14)$$

where, m is the tip mass, r is the radius of gyration of mass, and l is the distance between the attachment point and center of gravity of mass. The bending stiffness of messenger cable and circular frequency of the SBD are also denoted respectively by k_{ij} and $\omega_{s=1,2}$ (where $i, j = 1, 2, 3, \dots$).

The SBD has been designed by using Eqs. (10)-(14). The properties of the dampers have been given in Table 3. The damping ratio in Stockbridge damper is related to the logarithmic decrement of damping of messenger cable.

Table 3 Properties of the dampers

Parameters	SBD
mass ratio	0.022
Mass (kg)	9143.05
Frequency ratio	0.9784
Hysteresis damping constant	0.159
Logarithmic decrement of damping	0.5
Messenger cable length (m)	1.5
Location of SBD	Tower top

The considered Young's modulus, Poisson's ratio and density of SBD materials have been taken respectively 2.1×10^{11} N/m², 0.31 and 7900 kg/m³. To find better performance of damper, the parameters of the damper have been optimized using RSM based on BBD and PSO algorithm.

3.3 Design variables of Stockbridge damper and responses of structure

To minimize the maximum displacement, maximum standard deviation of displacement and frequency response of tower top of the OWT structure, the parameter of SBD like length of messenger cable (LMC), logarithmic decrement of damping (LDD) and diameter of messenger cable (DMC) have been selected as design variables whereas the mass of SBD has been considered as 2.22% of the first modal mass of OWT. To find an optimum SBD, the following objective functions were considered in the optimization.

$$J_1 = \min_i \parallel \max_t |TD(t)| \quad (15)$$

$$J_2 = \min_i \parallel \max_t |RMSD(t)| \quad (16)$$

$$J_3 = \min_i \parallel \max_t |FR(t)| \quad (17)$$

where i indicates the top of the tower, and $TD(t)$, $RMSD(t)$, and $FR(t)$ are the tower top displacement, root mean square displacement and frequency response of tower of structure.

The above objective function has been formulated as the following constrained optimization problem, where the constraints are the SBD parameters bounds.

DMC, LMC, and LDD

Minimize J subject to

$$DMC_{mc}^{min} \leq DMC_{mc} \leq DMC_{mc}^{max} \quad (18)$$

$$LMC_{mc}^{min} \leq LMC_{mc} \leq LMC_{mc}^{max} \quad (19)$$

$$LDD_d^{min} \leq LDD_d \leq LDD_d^{max} \quad (20)$$

4. Proposed optimization scheme: RSM based on Box-Behnken Design and particle swarm optimization

4.1 Box-Behnken Design in response surface methodology

The Response Surface Methodology (RSM) is one of the good approaches to approximate the observed data. Therefore, the RSM is convenient for developing, improving and analyzing problems and consists of data collection, modeling, and optimization (Myers *et al.* 2016).

It investigates the relationship between the design variables and response variables in an interest region. The relation between the design and response variables have

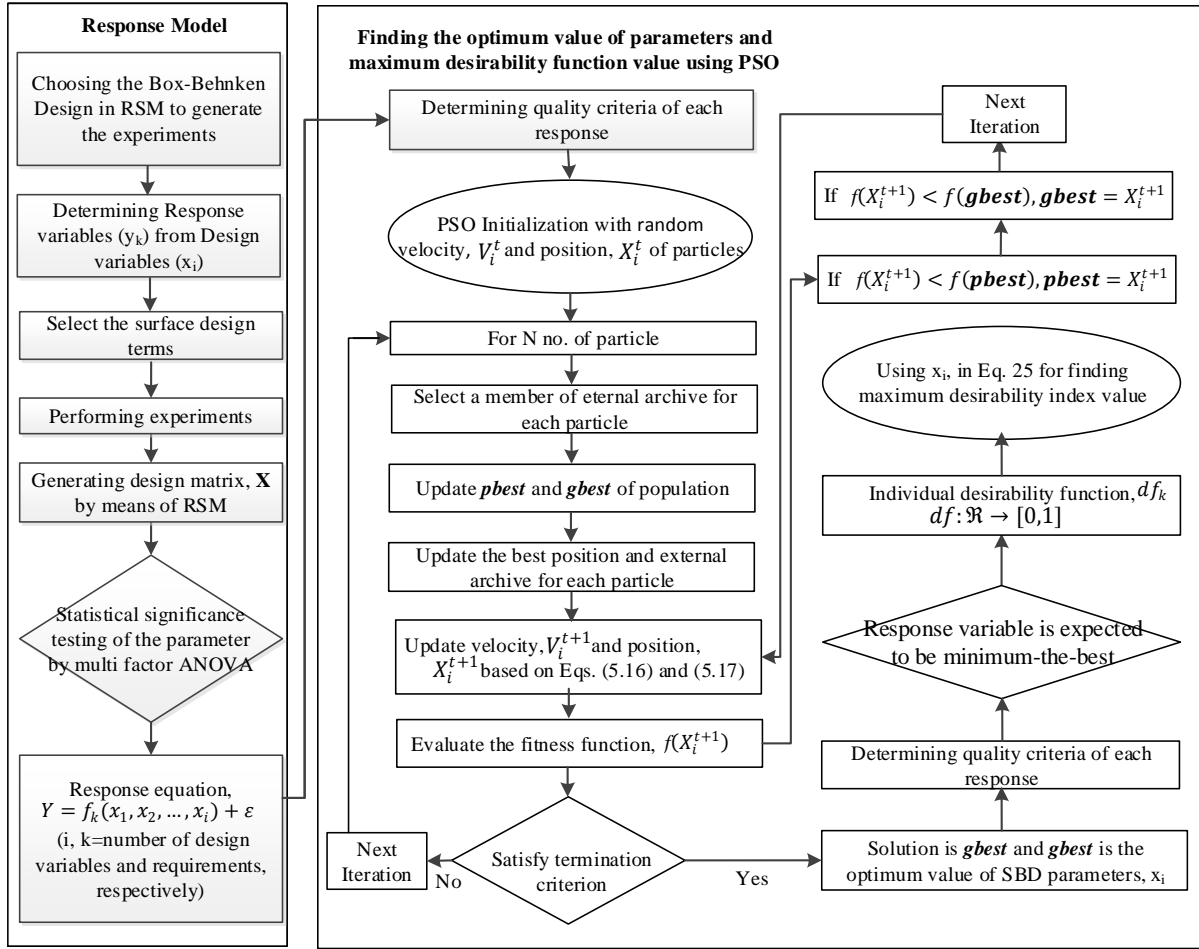


Fig. 5 Flow chart on optimization procedure employing RSM based on BBD, classical experimental design, and PSO algorithm

been expressed by the following equation.

$$Y = f_k(x_1, x_2, \dots, x_i) + \varepsilon, \text{ subject to } x \in \Lambda, \quad (21)$$

where Y is the response variables need to be minimized in the interest region of Λ , $x_{i=1 \text{ to } i}$ is the design variables need to be optimized in k number of experiment and ε is the error of the regression equation.

Usually, in the optimization process requires the designed experiments, coefficients of a statistical model, and predicting the response of output variable and checking the adequacy of the model. An experimental model has been developed based on a second order quadratic model for optimum SBD to correlate the structural response and is given in Eq. (22).

$$Y = b_0 + \sum_{i=1}^k b_i x_i + \sum_{i=1}^k b_{ii} x_i^2 + \sum_{i=1}^{k-1} \sum_{j>1}^k b_{ij} x_i x_j + \varepsilon \quad (22)$$

where b_0 is the value of fitted response at the center point of design, b_i, b_{ii}, b_{ij} is the coefficients of the linear effect, double interactions; x_i, x_j are the response variables and ε is error. The second-order model includes all the terms in the first-order model.

The Box-Behnken Design (BBD) is one of the designs of an experiment for numerical calculation of nonlinear model for the optimization process of variables. Each factor, or design variable, is placed at one of three equally spaced values, usually coded as $-1, 0, +1$. At least three levels are needed for the BBD experiment.

Here, Box-Behnken Design (BBD) has been utilized to find the combined effect of DMC, LMC and LDD of SBD on minimizing the maximum displacement, the RMSD, and frequency response amplitude of the structure.

The experimental data have been analyzed using statistical methods appropriate to the experimental design. The relation between the coded and actual values has been described by Eq. (23).

$$x_i = \left(\frac{X_i - X_0}{\Delta X_i} \right), i=1, 2, 3, \dots, k \quad (23)$$

where x_i and X_i are the coded and actual values of the design variable. X_0 is the actual value of the design variable at the center point, and ΔX_i is the step change of X_i .

Table 4 Box–Behnken design with actual and coded values for three factors and corresponding responses

Experiment	Actual and coded level of design variables			Responses		
	x_1	x_2	x_3	TD (m)	RMSD	FR (dB)
1	0.60(-1)	0.50(-1)	0.09(0)	0.269819	0.113799	10.1270
2	1.50(+1)	0.50(-1)	0.09(0)	0.260689	0.104824	10.0356
3	0.60(-1)	0.80(+1)	0.09(0)	0.266274	0.106826	10.0685
4	1.50(+1)	0.80(+1)	0.09(0)	0.261648	0.102990	10.0158
5	0.60(-1)	0.65(0)	0.06(-1)	0.268919	0.112378	10.1142
6	1.50(+1)	0.65(0)	0.06(-1)	0.266121	0.106223	10.0696
7	0.60(-1)	0.65(0)	0.12(+1)	0.263114	0.107169	10.0806
8	1.50(+1)	0.65(0)	0.12(+1)	0.260498	0.101742	9.9926
9	1.05(0)	0.50(-1)	0.06(-1)	0.265749	0.108830	10.0841
10	1.05(0)	0.80(+1)	0.06(-1)	0.268798	0.111827	10.1014
11	1.05(0)	0.50(-1)	0.12(+1)	0.262493	0.106719	10.0645
12	1.05(0)	0.80(+1)	0.12(+1)	0.260452	0.101042	9.9896
13	1.05(0)	0.65(0)	0.09(0)	0.258685	0.099654	9.9878
14	1.05(0)	0.65(0)	0.09(0)	0.258685	0.099654	9.9878
15	1.05(0)	0.65(0)	0.09(0)	0.258685	0.099654	9.9878

4.2 Desirability function analysis

The concept of desirability function analysis (DFA) is popularized by Derringer and Suich (1980), for the simultaneous multi-response optimization problems. In the DFA, each estimated response (e.g., the i th estimated response Y_i) has been transformed into a scale-free value, called individual desirability function (denoted as d_i (Y_i)) that are then amalgamated into a composite or overall desirability function. The composite desirability D , combined the individual desirability values. The value of individual or composite desirability remain between 0 and 1. When the response is out of acceptable limit, the corresponding desirability value will be 0.

When the response is in acceptable limit, the desirability will be 1 or closer to 1. Value of the response variable is expected to be minimum-the-best (MTB)-type, the individual desirability function in Eq. (24).

$$d_i(Y_i) = \begin{cases} 1 & \text{if } Y_i(x) \leq Y_{min} \\ \left(\frac{Y_i(x) - UV_{Y_i}}{Y_{min} - UV_{Y_i}}\right)^{\alpha_i} & \text{if } Y_{min} \leq Y_i(x) \leq UV_{Y_i}, \alpha_i \geq 0 \\ 0 & \text{if } Y_i(x) \geq UV_{Y_i} \end{cases} \quad (24)$$

When the response is out of acceptable limit, the corresponding desirability value will be 0. When the response is in acceptable limit, the desirability will be 1 or closer to 1, where UV_{Y_i} is the upper value of response variables, and to find the maximum composite desirability index value of design variables, the following Eq. (25) is used.

$$arg \max_{x_1, x_2, \dots, x_n} \left[\prod_{k=1}^m d f_k [f_k(x_1, x_2, \dots, x_n)]^k \right]^{\frac{1}{k}} \quad (25)$$

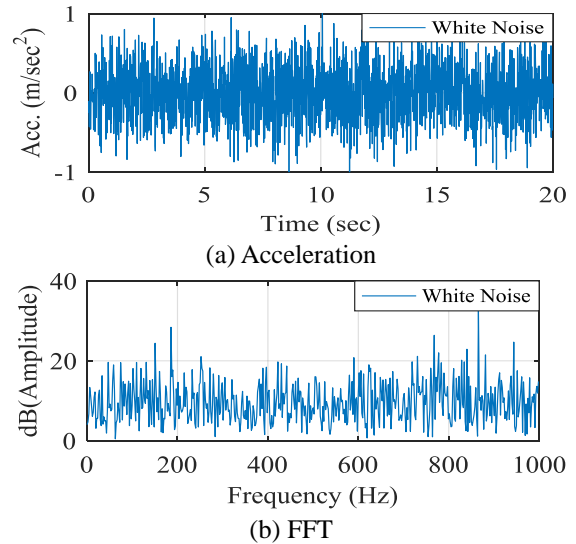


Fig. 6 Acceleration and FFT of white noise signal

4.3 Determination of optimum value and desirability function : Particle swarm optimization

The PSO algorithm as a meta-heuristic optimization technique which is utilized to find the optimum point of parameters of SBD. In the PSO, the solution of optimization problem has been denoted as particle. The particle changes its position and velocity gradually through tracking its own local and global location and in the whole swarm experience. After the origination of PSO, it has been successfully applied for optimization problem in many engineering problems (Leung *et al.* 2008, Leung and Zhang 2009, Chen *et al.* 2009). Tang *et al.* (2013) have applied the PSO approach to determine the structural damage. In this paper, the steps have been used to find the optimum point using PSO (see Fig. 5).

In the PSO approach, 100 number of particles has been involved, which has been initialized randomly in the search

Table 5 Quadratic model summary to check the adequacy

Response	SBD	
	Model Equation with coded coefficient	R ² (%)
y_1	$0.25869 - 0.00239x_1 - 0.00019x_2 - 0.00287x_3 + 0.0031x_1^2 + 0.00282x_2^2 + 0.00287x_3^2 + 0.001126x_1x_2 + 0.00004x_1x_3 - 0.00127x_2x_3$	95.25%
y_2	$0.09965 - 0.00304x_1 - 0.00143x_2 - 0.00282x_3 + 0.00361x_1^2 + 0.00384x_2^2 + 0.00361x_3^2 + 0.00128x_1x_2 + 0.00018x_1x_3 - 0.00216x_2x_3$	98.05%
y_3	$9.98785 - 0.03457x_1 - 0.01700x_2 - 0.03026x_3 + 0.03910x_1^2 + 0.03478x_2^2 + 0.03729x_3^2 + 0.00966x_1x_2 - 0.01088x_1x_3 - 0.02306x_2x_3$	99.65%

Table 6 Degree of reliability and precision value of full quadratic model

Response	Unit	Sources	Sum of squares	DOF	Mean Square	F-value	P-value
TD	m	Model	0.000207	9	0.000023	11.14	0.008*
		Residual error	0.000010	5	0.000002		
		Sum	0.021711	14			
RMSD		Model	0.000311	9	0.000035	28	0.001*
		Residual error	0.000006	5	0.000001		
		Sum	0.031710	14			
FR	dB	Model	0.035391	9	0.003932	158.65	<0.001*
		Residual error	0.000124	5	0.000025		
		Sum	0.035515	14			

space of an objective function. These particles have been referred to as a swarm. Each particle of the swarm represents a potential solution to the optimization problem.

The 100 particles in 30 iterations have been associated with a position vector, X_i^t , and a velocity vector, V_i^t , that shown as following Eqs. (26) and (27).

$$X_{i=100}^t = \{x_{i1}^t, x_{i1}^t, \dots, x_{ik}^t\} \quad (26)$$

$$V_{i=100}^t = \{v_{i1}^t, v_{i1}^t, \dots, v_{ik}^t\} \quad (27)$$

The particle flies through the solution space and its position is updated based on its velocity, the best position particle ($pbest$) and the global best position ($gbest$) that swarm has visited the first iteration as

$$V_{i=100}^{t+1} = \{w^t \times V_i^t + c_1 r_1 (pbest_i^t - X_i^t) + c_1 r_1 (gbest^t - X_i^t)\} \quad (28)$$

$$X_{i=100}^{t+1} = X_i^t + V_i^{t+1} \quad (29)$$

where r_1 and r_2 are two uniform random have been taken as 0.1 and 1.1; the cognitive (c_1) and social scaling (c_2) parameters have been considered as 2; and the inertia factor (w^t) has been used to discount the previous velocity of particle preserved and has been considered as 1.49.

5. Preparation of response models with design variables of SBD

5.1 Analysis points and structural responses

The design of the experiment has been configured based

on Response Surface Methodology (RSM) based on Box-Behnken Design (BBD) to investigate the effect of factors on the responses. For finding an optimum SBD, the parameters like length of messenger cable (LMC), logarithmic decrement of damping (LDD) and diameter of messenger cable (DMC) have been selected as design variables when the structural response like tower top displacement (TD), RMSD and frequency response (FR) of tower top have been considered as response variables. Choosing of design variable is an engineering judgment.

This is depending on every engineer or researcher knowledge. In this manuscript, the range of LMC, LDD, and DMC of SBD has been chosen between 0.60 m to 1.50 m, 0.50 to 0.80 and 0.06 m to 0.12 m. The design of experiment (DOE) has been made at total 15 experimental points composed of 3 center points and 12 axial points. To complete these optimizations, the analysis has been performed for fifteen times. However, the analysis for optimization has been performed under an artificially generated white noise signal, which had 4000 load steps and 0.005 time steps. The white signal and its FFT is given in Fig. 6.

The corresponding analysis point and structural responses for each structural model have been illustrated by Table 4.

The proposed second-degree polynomial has been fitted to the data presented in Table 4 using multiple linear regressions to determine the optimum value that resulted in the maximum responses of structure under white signal.

The effects of LMC, LDD and DMC of SBD in vibration reduction are quantitatively evaluated using response surface curves.

Table 7 Parameter configuration for individual desirability function

Response	Goal	Target	Upper limit	Relative weight
TD (m)	Minimum	0.2585	0.27	1
RMSD	Minimum	0.0994	1.138	1
TFR (dB)	Minimum	9.965	10.127	1

Table 8 Proposed optimum value of parameters of SBD and composite desirability function value

Input/output variables	SBD		
	Optimal Point (uncoded)	Individual desirability index	Composite desirability index
LMC, (m)	1.26364	0.978	0.977
LDD	0.706061	0.978	
DMC, (m)	0.107879	0.976	

5.2 Model adequacy and analysis of variance

The predicted values of LMC, LDD and DMC and the coefficient of determination (R^2) using regression equation is given in Table 5. The quality of fit of the polynomial model equation is expressed by the coefficient of determination, R^2 . Moreover, the coefficient of determination (R^2) is given in Table 5. From the Table 5, the corresponding coefficients of determination have been found 0.9525, 0.9805 and 0.9965, which are indicated that the model adequately represented the real relationship between the variables under consideration. Also, the values of R^2 illustrates about the percentage of variability of the model. The significance of the fitted of the second-order polynomial for the LMC, LDD and DMC have been assessed by carrying out analysis of variance (ANOVA) and the results have been given in Table 6, as well.

The coefficients of variation value have been illustrated by the P value. The P value of the response variables have been found 0.008, 0.01 and <0.001 respectively for the top displacement, standard deviation of displacement and frequency response of structure. The value of P indicates the degree of reliability of the regression model (Montgomery 2005, Mason *et al.* 1989). Also, the adequate precision value, have been illustrated by the F-value. When the value of F is greater than 4, then it will be durable (Cao *et al.* 2009). Here, all of the F-value is found as greater than 4.

5.3 Response surface plot of design and response variables

In order to show the effects of independent variables on the dependent one, the 3D response surface curves have been drawn. The surface plots have been drawn by considering two variables constant and varying the others within the experimental range. The response surfaces present the effect of DMC, LMC and LDD of the SBD on vibration reduction.

The relationship between the design and response variables have been presented by a graphical form in Figs. 7 and 8. The three-dimensional response surface plots illustrate the interactive effects of the DMC, LMC and LDD of the damper on vibration reduction. Likewise, the combined effects of DMC, LMC and LDD of damper on the TD, RMSD and FR have been presented by Figs. 7 and 8.

The maximum predicted values have been indicated by the concave surface plot. The figures show the effect of LMC, LDD and DMC on TD of OWT. The higher displacement response is found with the rising of LMC, LDD and DMC value; however, for a lower value of parameters, the displacement will be decreased but until a point and that can be shown from contour map. Similarly, the effects of LMC, LDD and DMC on RMSD and FR, are found similar.

5.4 Determination of optimum value and the desirability function

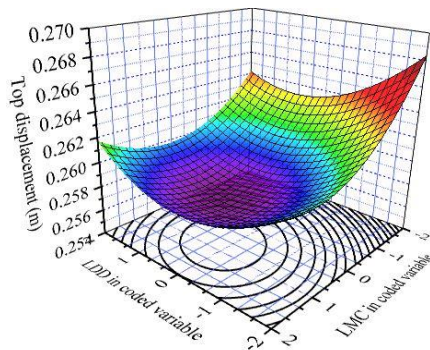
In order to find the optimum value of design parameters, the PSO approach has been utilized. Moreover, the desirability function has been used to find the maximum desirability of design variables. For the SBD parameter optimization cases, tower top maximum displacement, RMSD, frequency response, has been targeted to minimize.

The response goal of optimization and parameter limits for different responses of SBD have been given in Table 7.

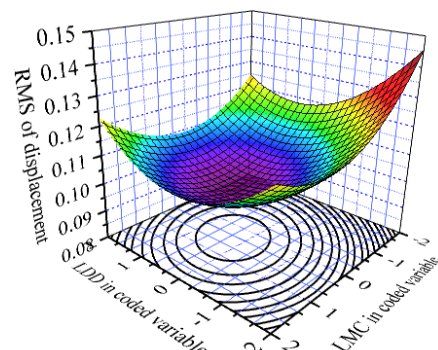
Here, three responses are competing for each other on the basis of three design variables of TD, RMSD and FR of SBD. The optimal design point for proposed criteria, individual and composite desirability values are given in Table 8.

The Figs. 8(b), 8(d) and 8(f), illustrates that the maximum desirability could be found up to a range of value. Then the desirability will change with the changing of design variables values. The corresponding optimum value of parameters and the desirability index of design variables is given in Table 9.

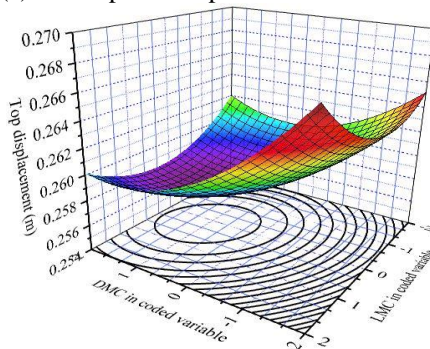
The predicted responses and measured responses are given in Table 9. The results are obtained from three and maximum frequency response amplitude (10.180 dB) of the structure along with the individual desirability of 0.978, 0.978 and 0.976 respectively for SBD parameters. Replications demonstrated that the average of the maximum top displacement (0.2505 m); maximum RMSD (0.09413). Moreover, from the obtained results, the predicted values are found respectively 0.2578m, 0.0984 and 10.18021dB. The differences of predicted responses and measured responses are found respectively 2.83%, 4.35% and 2.08% respect to the TD, RMSD, and FR. The low difference between the predicted and measured values from these experiments indicates the validity of response model.



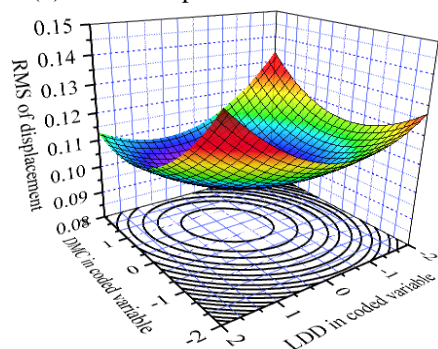
(a) TD response respect to LDD and LMC



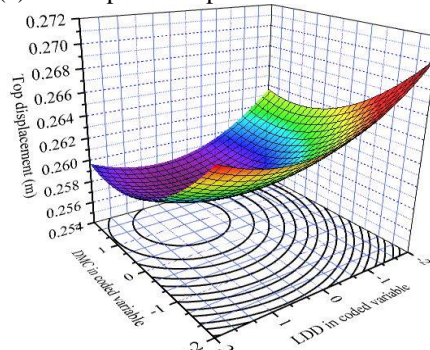
(b) RMSD respect to LDD and LMC



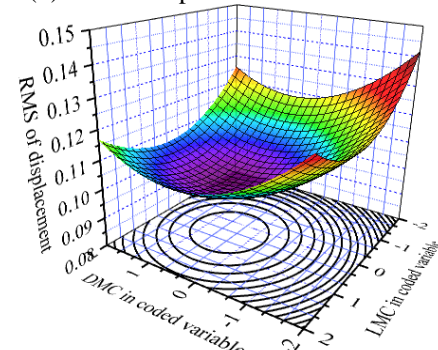
(c) TD response respect to DMC and LMC



(d) RMSD respect to DMC and LMC



(e) TD response respect to DMC and LDD



(f) RMSD respect to DMC and LDD

Fig. 7 Effects of design variables on tower top displacement and RMSD

Table 9 Best global solution for obtaining the SBD parameters

Response	RS model	S. model	Difference
TD (m)	0.2578	0.2505	2.83%
RMSD	0.0984	0.09413	4.35%
FR (dB)	9.9674	10.18021	2.08%

RS: Response surface; S: Structural

5.5 Best fitness convergence rate by PSO

The results of the fitness values (maximum desirability) versus the number of iteration by PSO is plotted in Fig. 9. Fig. 9 illustrates that the fitness value is increased with number of iteration. Moreover, after the fifteen iterations, the fitness values remained same. Here, the fitness values are considered as composite desirability index value.

6. Dynamic responses of offshore wind turbine with the optimized and non-optimized SBD

6.1 Base excitations for structural responses

To evaluate the effectiveness of the SBD system, the considered structure are analyzed under three recorded earthquake loads like El Centro 1940NS, Northridge 1994

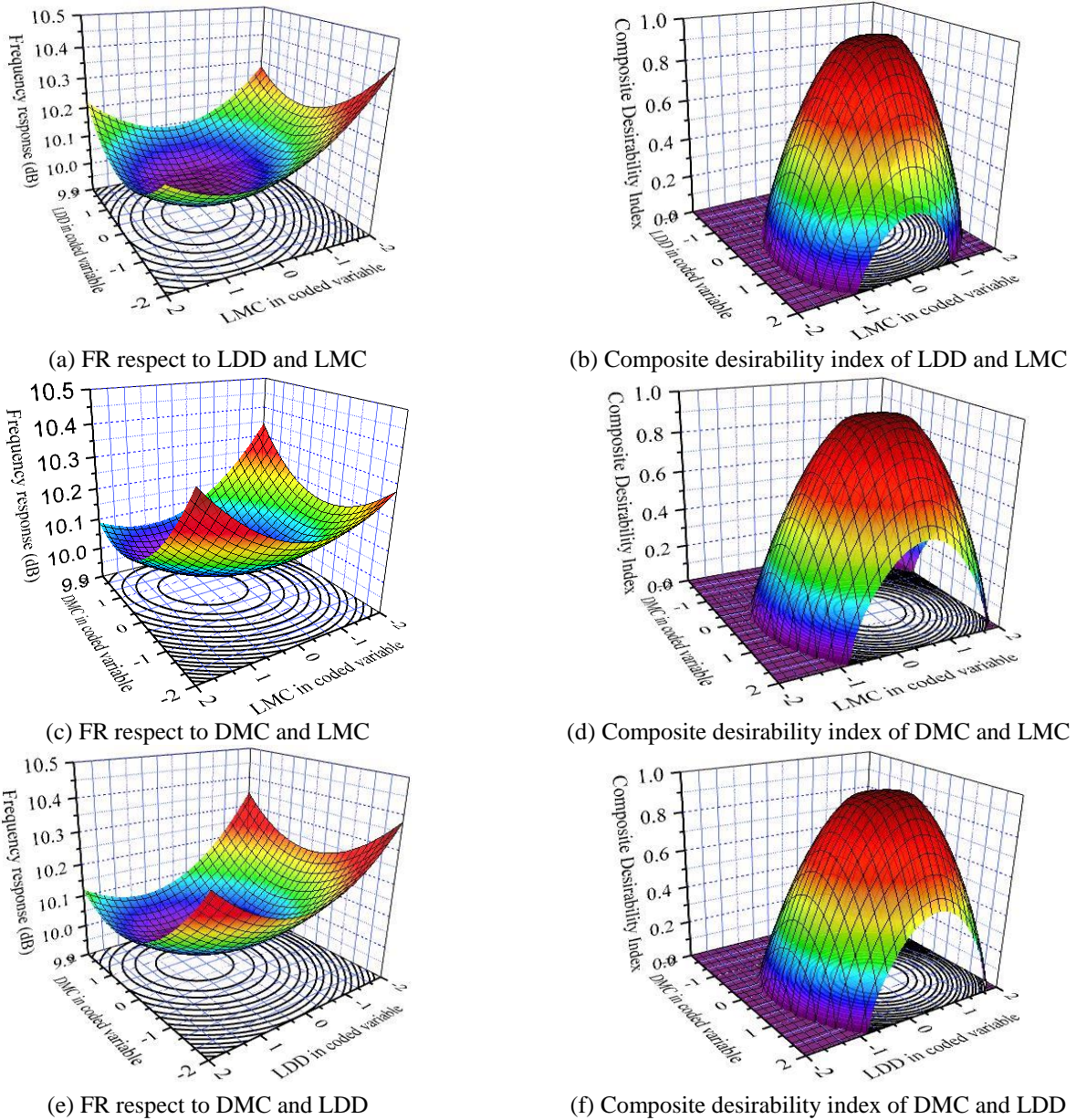


Fig. 8 Effects of design variables on frequency response and Composite desirability index plot of design variables

and Tabas 1978 earthquake. The time steps and PGA of the three earthquakes are respectively as 0.02 s, 0.01 s, 0.01 s and 0.348 g, 0.343 g, 0.0899 g. Here, all of the accelerations of signal are executed as a time history. Therefore, the motive for applying several earthquakes to check the behavior of OWT and the effectiveness of damper under different earthquakes whose contain various distinctive frequencies.

6.2 Displacement responses under earthquake loads

Fig. 10 illustrates the time series responses at the top of the tower with and without SBD under the selected earthquake excitations. Based on Figs. 10(a), 10(c) and 10(e), it is clearly visible that the minimizing amount of

maximum tower top displacement responses for the RSM based on BBD and PSO optimized SBD are 41.83%, 48%, and 42% respectively under the El Centro, Northridge and Tabas earthquakes successively with respect to the uncontrolled structure. Moreover, from the Figs. 10(a), (c) and (e), it is clearly seen that the minimizing amount of maximum tower top displacement responses for the non-optimized SBD are 30.05% under El Centro, 29.29% under Northridge, and 30.04% under Tabas earthquake successively with respect to the uncontrolled structure. The structure with RSM based on BBD and PSO optimized SBD shows 11.78%, 18.71%, and 11.6% less response during the earthquakes than the structure with non-optimized damper.

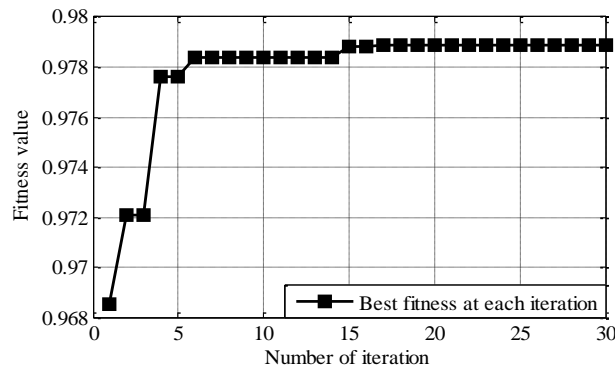
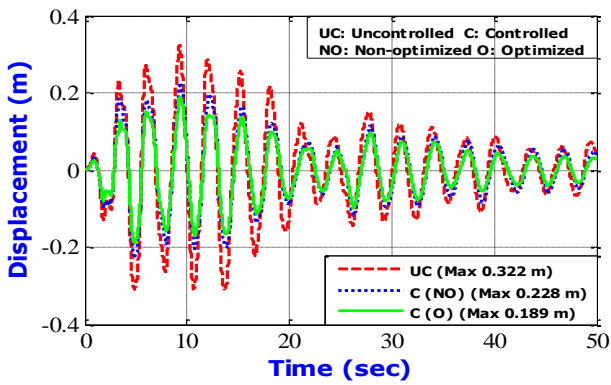
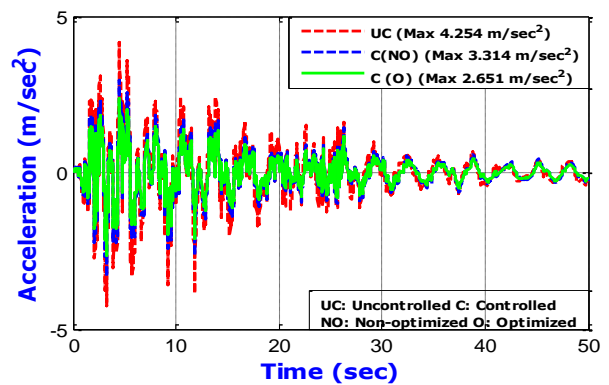


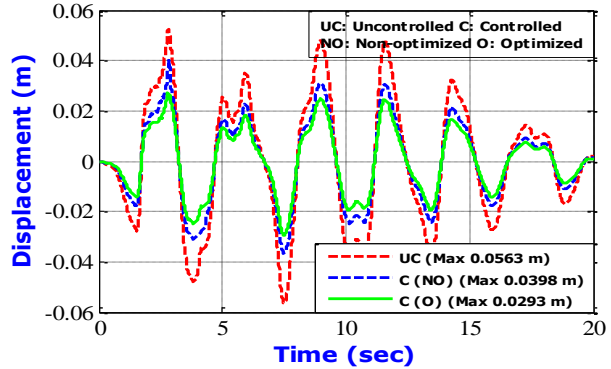
Fig. 9 Best fitness convergence rate by PSO



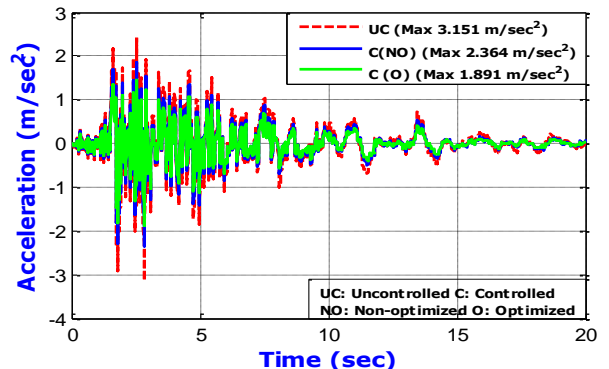
(a) Top displacement (El Centro earthquake)



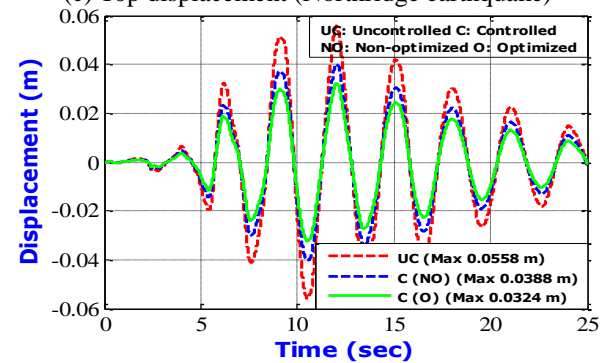
(b) Top acceleration (El Centro earthquake)



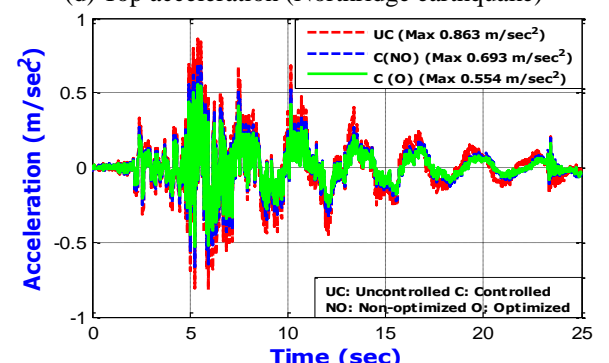
(c) Top displacement (Northridge earthquake)



(d) Top acceleration (Northridge earthquake)



(e) Top displacement (Tabas earthquake)



(f) Top acceleration (Tabas earthquake)

Fig. 10 Time history responses (displacements and accelerations) of structure under earthquake loads

Table 10 Frequency domain responses of OWT under earthquake loads

Structural model	El Centro		Northridge		Tabas	
	Amplitude (dB)	Reduction rate (%)	Amplitude (dB)	Reduction rate (%)	Amplitude (dB)	Reduction rate (%)
Uncontrolled	12.15	-	8.56	-	10.75	-
Controlled (NO)	7.90	33.3	5.98	30.14	7.54	29.86
Controlled (O)	7.16	41.07	5.38	37.15	6.44	40.09

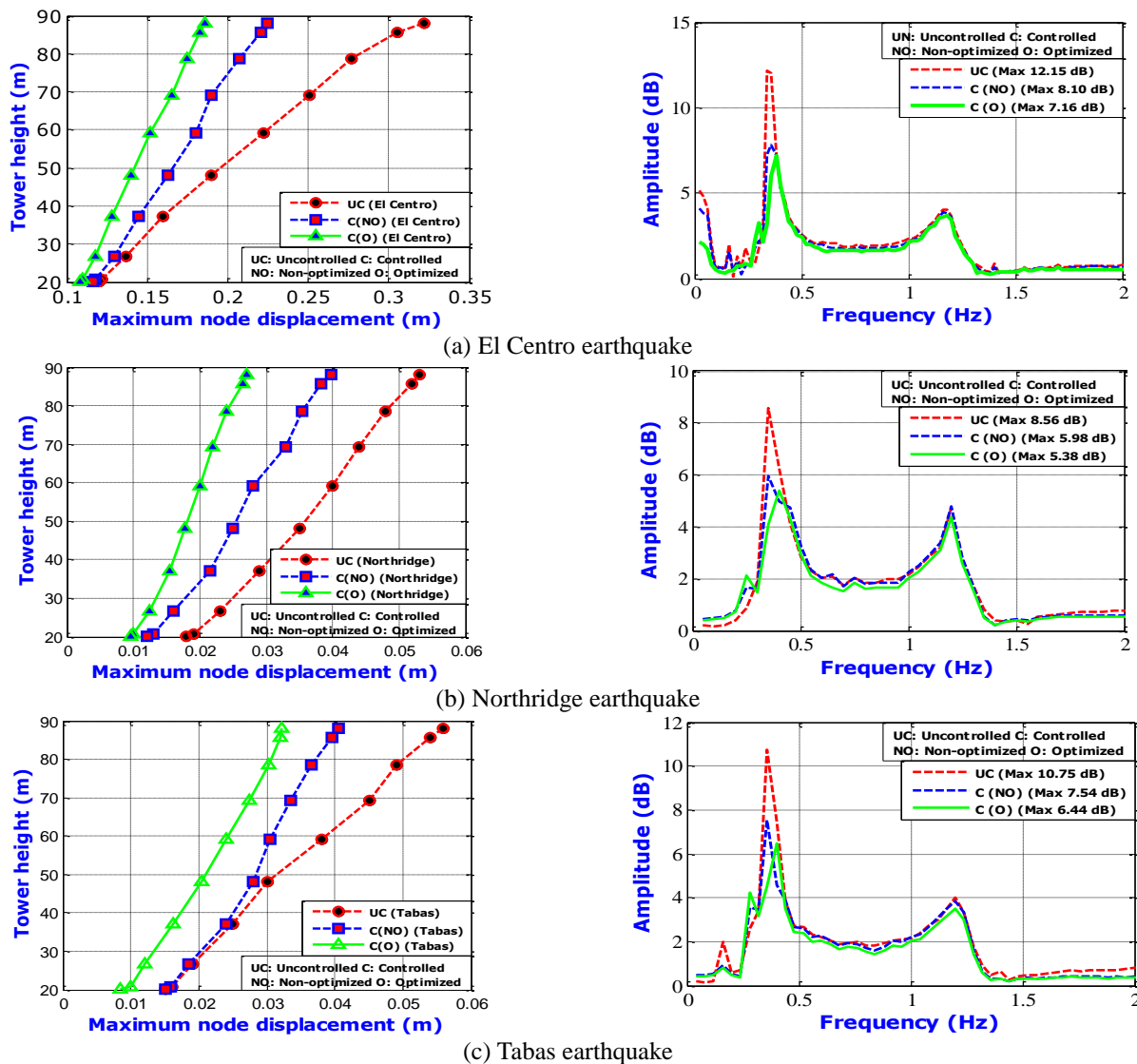


Fig. 11 Lateral displacement of tower of OWT and Frequency domain responses of OWT under earthquake loads

On the other hand, based on Figs. 10(b), 10(d) and 10(f), it is clearly seen that the minimizing amount of maximum tower top acceleration responses for the optimized SBD are 37.68% under El Centro, 39.99% under Northridge and 35.81% under Tabas earthquake successively with respect to the uncontrolled structure. Moreover, from the Figs. 10 (b), 10(d) and 10(f), it is clearly seen that the minimizing amount of maximum tower top acceleration responses for the non-optimized SBD are 22.10%, 24.98%, and 19.70% respectively under the El Centro, Northridge and Tabas

earthquakes successively with respect to the uncontrolled structure. The structure with RSM based on BBD and PSO optimized damper shows 15.58%, 15.01% and 16.11% more effective during the earthquakes than the structure with non-optimized damper. Meanwhile, the reduction percentages of acceleration are less than displacement decrement rates, the decline values are reasonable for acceleration response, which indicates the efficiency of the SBD.

6.3 Lateral displacement and frequency responses under earthquake loads

The lateral displacement pattern of tower of OWT during the earthquakes is shown in Fig. 11 (left). In addition, the maximum lateral displacement along with the tower height of the structure has been evaluated for the applied ground motions. Fig. 11 (left) demonstrates the responses of the tower with and without SBD under the selected ground excitations. The top lateral displacement is more compared to the tower bottom of the structure under all three earthquake motions, which is expectedly behaving like a cantilever beam.

The frequency response of any structure carries an important role for its high amplitude during the earthquake signal. Also, the frequency response helps researchers to understand how effective the damper is in controlling and resonance of structure. The FRs are have been checked for the same ground motions. The frequency responses of the structure with and without damper are given in Fig. 11 (right).

Fig. 11 (FFT curves) illustrates the frequency responses under three applied earthquake excitations at the top of the tower associated with the SBD. It is clearly seen that the fundamental first mode of OWT is controlling by the SBD. This mode contains the maximum amplitude of the uncontrolled and controlled structure. The reduced rates are given in Table 10. However, the Table 10 illustrates the effectiveness of SBD and optimized SBD. Moreover, the Table 10 illustrates the optimized SBD reduces more frequency amplitudes than non-optimized SBD. Under the applied earthquakes, the structure with RSM based on BBD and PSO optimized damper shows 7.77%, 7.01%, and 10.23% less frequency response than the structure with non-optimized damper.

6.4 Standard deviation of displacement

In order to grasp the attributes of displacement response and effectiveness of SBD in decreasing the responses, furthermore, the standard deviation of displacements has been determined. The standard deviation of displacement is referred as root mean squared displacement (RMSD). The standard deviation of displacement of OWT is determined by Eq. (30).

$$\text{RMSD} = \sqrt{\frac{1}{N} \sum_{n=1}^N |\text{disp}_n|^2} \quad (30)$$

The outcome of the RMS value of displacement responses with and without SBD of the structure under three seismic excitations are shown in Fig. 12 that illustrates that the structure with damper shows a better response than the structure without a damper.

Fig. 12 also illustrates that the reduction of RMSD of OWT with optimized damper shows more than the structure with non-optimized damper. Based on Fig. 12, the reduction percentages of RMS at the tower top displacement with the optimized and non-optimized damper are around 42.4%, 48%, 41.67% and 29.6%, 34.01%, 30.40% with respect to the uncontrolled structure due to El Centro, Northridge and Tabas

earthquakes successively. Thus, the analysis results serve the main concern of reducing vibration of OWT under earthquakes through SBD and optimized SBD. The structure with RSM based on BBD and PSO optimized damper is 12.8%, 13.99% and 11.27% more effective during the earthquakes than the structure with non-optimized damper.

6.5 Shear forces and flexural responses of tower

The shear forces of tower have been plotted respect to the nodes and given in Fig. 13 (left). The nodes 10 and 1, respectively reflect the tower top and bottom. The shear forces are found almost randomly fluctuated from top to bottom of the tower because of different picks of input signals. Under the El Centro earthquake, 2.85 MN shear force is found for uncontrolled tower, while the structure with optimized and non-optimized SBD shows respectively 2.51 MN and 2.61 MN. Moreover, the structure with and without damper shows respectively 2.315 MN and 2.44 MN under the Northridge earthquake. And the uncontrolled structure shows 1.56 MN under the Tabas earthquake while for controlled one, shear force is found 1.21 MN and 1.39 N respectively for optimized and non-optimized damper. Moreover, the flexural response of structure also evaluated and shown in the Fig. 13 (right). The maximum moments of the tower is observed at the bottom respectively for the uncontrolled and controlled structure, however, the structure with optimized damper shows minimum response than other model. The minimum moments of tower with optimized SBD are 134.5 MN-m, 112 MN-m and 89 MN-m respectively for El-Centro, Northridge and Tabas earthquake. Moreover, the maximum moments are found for uncontrolled structure under the ground signals. The reduction of shear force and moment is meaning that SBD is effective in terms of vibration reduction of wind turbine tower.

7. Conclusions

The Stockbridge Damper (SBD) is very well-known as passive damper device in transmission line area and slender structure. In this paper, the SBD is introduced to the field of vibration control of Offshore Wind Turbine (OWT). The installed SBD in OWT, successively reduced the earthquakes responses.

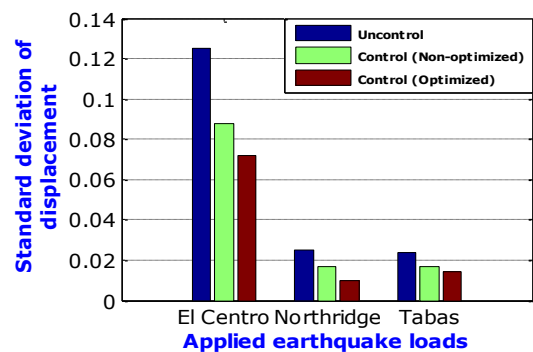


Fig. 12 Standard deviation of displacement under the earthquakes

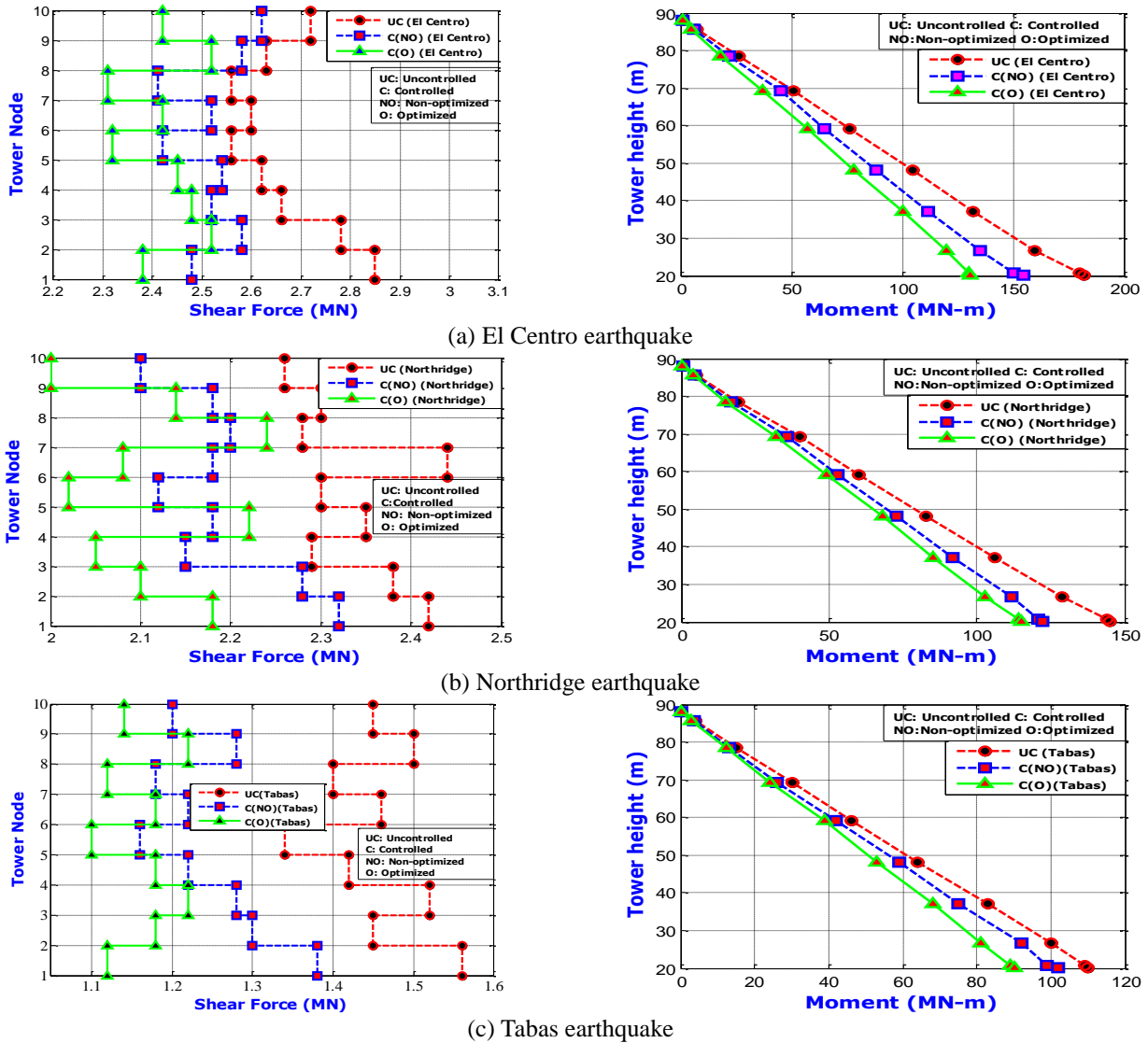


Fig. 13 Shear forces and Flexural responses of tower for earthquake loads

Moreover, the RSM based on BBD and PSO optimization approach provides an effective damper. The effectiveness of optimized damper is evaluated by comparing the response of structure with non-optimized damper. The SBD system has been employed to control the vibration of the structure under the earthquake loads based on the modal participation factor. The SBD has been designed to mitigate the first fundamental mode of the uncontrolled structure. Based on the analyzed results, the magnetic parts of results are given as conclusions at below:

- The application of the SBD system along with the jacket supported OWT is new vibration control system for this kind of ocean structures.
- The optimization approach is used in this paper is apparently new for this damper optimization.
- According to the time domain responses, lateral displacement and RMS results, the presence of SBD in OWT, can significantly reduce the tower top displacement more than 29.29% of the structure under

the applied seismic loads. Similarly, the SBD can reduce the peak acceleration responses, shear forces and flexural responses of the tower due to the applied control system.

- Through the FFT outcomes, the amplitude mitigation rates for employed ground motions are greater than 29.86% for the first mode with respect to the uncontrolled structure. It indicates the proficiency of the SBD system incorporates the structure.
- Moreover, the structure with the optimized damper shows 18.71% less displacement response during earthquakes. Similarly, the structure with the optimized SBD is more effective than the non-optimized damper respect to the peak acceleration responses, frequency response, shear forces and flexural responses of the tower due to the applied control system.

Acknowledgments

This work has been supported by Industry Technology Innovation Program of the Korea Institute of Energy Technology Evaluation and Planning (KETEP) grant financial resource from the Ministry of Trade, Industry & Energy, Republic of Korea (No. 2015030023760) and supported by Basic Science Research Program through the National Research Foundation of Korea (NRF) funded by the Ministry of Education (No. NRF-2016R1C1B1013481).

References

- Alkmim, M.H., De Morais, M.V.G. and Fabro, A.T. (2016), "Vibration reduction of wind turbines using tuned liquid column damper using stochastic analysis", *J. Phys. Conference Series*, **744**(1), 012178.
- Barry, O.R. (2014), "Vibration modeling and analysis of a single conductor with Stockbridge dampers", Ph.D. Dissertation, University of Toronto, Canada.
- Barbieri, N. and Barbieri, R. (2012), "Dynamic analysis of Stockbridge damper", *Adv. Acoust. Vib.*, **2012**, Article ID: 659398.
- Bezerra, M.A., Santelli, R.E., Oliveira, E.P., Villar, L.S. and Escalera, L.A. (2008), "Response surface methodology (RSM) as a tool for optimization in analytical chemistry", *Talanta*, **76**(5), 965-977.
- Box, G.E. and Behnken, D.W. (1960), "Some new three level designs for the study of quantitative variables", *Technometrics*, **2**(4), 455-475.
- Brodersen, M.L. and Høgsberg, J. (2014), "Damping of offshore wind turbine tower vibrations by a stroke amplifying brace", *Energy Procedia*, **53**(2014), 258-267.
- Cao, G., Ren, N., Wang, A., Lee, D.J., Guo, W., Liu, B., Feng, Y. and Zhao, Q. (2009), "Acid hydrolysis of corn stover for biohydrogen production using *Thermoanaerobacterium thermoanaerobacterium* W16", *Int. J. Hydrogen Energ.*, **34**(17), 7182-7188.
- Chang, S., Sun, W., Cho, S.G. and Kim, D. (2016), "Vibration Control of Nuclear Power Plant Piping System Using Stockbridge Damper under Earthquakes", *Sci. Technol. Nuclear Install.*, **2016**, Article ID. 5014093.
- Chen, J., Peng, W., Ge, R. and Wei, J. (2009), "Optimal design of composite laminates for minimizing delamination stresses by particle swarm optimization combined with FEM", *Struct. Eng. Mech.*, **31**(4), 407-421.
- Den Hartog, J.P. (1947), *Mechanical vibrations*, McGraw-Hill, New York.
- Derringer, G. and Suich, R. (1980), "Simultaneous optimization of several response variables", *J. Qual. Technol.*, **12**(4), 214-219.
- Dos Santos, J.M.M. (2015), "Modelling and analysis of wind-excited vibrations of transmission lines", Ph.D. Dissertation, University of Porto.
- Ferreira, S.C., Bruns, R.E., Ferreira, H.S., Matos, G.D., David, J. M., Brandao, G.C. and Dos Santos, W.N.L. (2007), "Box-Behnken design: an alternative for the optimization of analytical methods", *Analytica Chimica Acta*, **597**(2), 179-186.
- Jaksic, V., Wright, C.S., Murphy, J., Afeef, C., Ali, S.F., Mandic, D.P. and Pakrashi, V. (2015), "Dynamic response mitigation of floating wind turbine platforms using tuned liquid column dampers", *Phil. T. R. Soc. A.*, **373** (2035).
- Jeon, S.H., Seo, M.W., Cho, Y.U., Park, W.G. and Jeong, W.B. (2013), "Sloshing characteristics of an annular cylindrical tuned liquid damper for spar-type floating offshore wind turbine", *Struct. Eng. Mech.*, **47**(3), 331-343.
- Kasap, H. (2012), "Investigation of Stockbridge dampers for vibration control of overhead transmission lines", Ph.D. Dissertation, Middle East Technical University.
- Khan, A., Do, J. and Kim, D. (2016), "Cost effective optimal mix proportioning of high strength self-compacting concrete using response surface methodology", *Comput. Concrete*, **17**(5), 629-638.
- Lee, G.N., Kim, D.H. and Lee, Y.J. (2015), "Dynamic reliability analysis of offshore wind turbine support structure under earthquake", *Proceedings of the 2015 World Congress on Advances in Civil, Environmental, and Materials Research (ACEM15)*, Incheon, South Korea, August.
- Leung, A.Y., Zhang, H., Cheng, C.C. and Lee, Y.Y. (2008), "Particle swarm optimization of TMD by non-stationary base excitation during earthquake", *Earthq. Eng. Struct. D.*, **37**(9), 1223-1246.
- Leung, A.Y.T. and Zhang, H. (2009), "Particle swarm optimization of tuned mass dampers", *Eng. Struct.*, **31**(3), 715-728.
- Mason, L.R., Gunst, R.F. and Hess, J.S. (1989), *Statistical design & analysis of experiments*, Wiley, New York.
- Montgomery, D.C. (2005), *Design and analysis of experiments*, (6th Ed.), John Wiley & Sons Inc, New York.
- Mousavi, S.A., Zahrai, S.M. and Bargi, K. (2012), "Optimum geometry of tuned liquid column-gas damper for control of offshore jacket platform vibrations under seismic excitation", *Earthq. Eng. Eng. Vib.*, **11** (4), 579-592.
- Myers, R.H., Montgomery, D.C. and Anderson-Cook, C.M. (2016), *Response Surface Methodology: process and product optimization using designed experiments*, John Wiley & Sons.
- Navarro Canales, C., Lara López, A., Colín Venegas, J., Razo-García, J. and Aguilera-Cortés, L.A. (2008), "Optimal design of Stockbridge dampers", *Ingeniería Mecánica, Tecnología Y desarrollo*, **2**(6), 193-199.
- Rahman, M.S., Islam, M.S., Do, J. and Kim, D. (2017), "Response surface methodology based multi-objective optimization of tuned mass damper for jacket supported offshore wind turbine", *Struct. Eng. Mech.*, **63**(3), 303-315.
- Roderick, C. (2012), "Vibration reduction of offshore wind turbines using tuned liquid column dampers", Master Thesis, University of Massachusetts Amherst, United State.
- Sepehri, A., Daneshmand, F. and Jafarpur, K. (2012), "A modified particle swarm approach for multi-objective optimization of laminated composite structures", *Struct. Eng. Mech.*, **42**(3), 335-352.
- Shariatmadar, H. and Razavi, H. (2014), "Seismic control response of structures using an ATMD with fuzzy logic controller and PSO method", *Struct. Eng. Mech.*, **51**(4), 547-564.
- Song, H., Damiani, R., Robertson, A. and Jonkman, J. (2013), "A new structural-dynamics module for offshore multimember substructures within the wind turbine computer-aided engineering tool FAST", *Proceedings of the 23rd International Offshore and Polar Engineering Conference. International Society of Offshore and Polar Engineers*, Anchorage, Alaska, June.
- Soto-Pérez, L., López, V. and Hwang, S.S. (2015), "Response Surface Methodology to optimize the cement paste mix design: Time-dependent contribution of fly ash and nano-iron oxide as admixtures", *Mater. Des.*, **86**, 22-29.
- Stockbridge, G.H. (1925), "Vibration damper," Patent No. 1675391, USA Patent Office.
- Tang, H., Zhang, W., Xie, L. and Xue, S. (2013), "Multi-stage approach for structural damage identification using particle swarm optimization", *Smart Struct.Syst.*, **11**(1), 69-86.
- Urushadze, S., Pirner, M., Pospíšil, S. and Kral, R. (2012), "Experimental and numerical verification of vortex-induced vibration of hangers on the footbridge", *Proceedings of the 18th International Conference of Engineering Mechanics*, Svratka,

Czech Republic, May.

- Vorpahl, F., Popko, W. and Kaufer, D. (2011), "Description of a basic model of the UpWind reference jacket" for code comparison in the OC4 project under IEA Wind Annex XXX", *Fraunhofer Institute for Wind Energy and Energy System Technology (IWES)*, Bremerhaven, Germany.
- Wagner, H., Ramamurti, V., Sastry, R.V.R. and Hartmann, K. (1973), "Dynamics of Stockbridge dampers", *J. Sound Vib.*, **30**(2), 207-220.
- Wang, S.Q. and Li, N. (2013), "Semi-active vibration control for offshore platforms based on LQG method", *J Mar. Sci. Technol.*, **21** (5), 562-568.

CC